This file includes:

- Supplementary text
- Tables S1-S3
- Figures S1 to S7

Supplemental Methods:

Climate projections

A combination of 8 projections were used from 4 different global change models (GCMs) at two relative concentration pathways (RCPs). The RCPs chosen were 4.5 and 8.5, the former representing an emissions-controlled future, while the latter represents an uncontrolled emissions future. The particular combination is based on recommendations from Pierce et al. 2016. The LANDIS model utilizes the following climatological variables: daily precipitation (figure S1 and S2), daily maximum temperature (figure S3), daily minimum temperature, daily average windspeed, and daily average wind direction that are averaged across the Level II EPA ecoregions in the study area.

Forest succession

NECN (v6.5) simulates both above and belowground processes, tracking C and N through multiple live and dead pools, as well as tree growth (as net primary productivity--a function of age, competition, climate, and available water and N). Soil moisture, as well as movement across the dead pools: wood and litter deposition and decomposition, soil accretion and decomposition are based on the CENTURY soil model (Parton et al. 1983, Scheller et al. 2011). Carbon estimates by pool were validated against Wilson et al. (2013) at the ecoregion level, where the model overestimated total C for only one region but was within one standard deviation for all others (see supplemental figure S4). Forest growth estimates using the climate data for year 2010-2015 for the region were calibrated against the MODIS 17a3 product annual mean for 2000 – 2015 (Figure S5). Reproductive success is dependent on temperature and water.

Fire modeling

The SCRPPLE extension (v2.1) models ignitions by drawing the number of ignitions from a zero-inflated Poisson distribution and allocates them across the landscape with a weighted ignition surface for each type of fire modeled (Scheller et al. 2019). The weather influence on fire is based on the Fire Weather Index (FWI) measures created by the Canadian Fire Prediction System (1992). There are three categories of fires that can be modeled: lightning, accidental (i.e., human started), and prescribed fire. The extension also includes the ability to explicitly set fire suppression effort levels across the landscape as well as by ignition type, where the suppression parameter reduces the probability of fire spread from one cell to another. Effort levels can range from 0 to 3, where 0 is no suppression attempted, to 3 which represents high effort and was designed to mimic current suppression efforts in the Basin (Figure S6). However, suppression effectiveness can be limited by weather as well, a maximum wind speed parameter can limit suppression to days only when resources can be deployed safely. That parameter was set at wind speeds of 11 meters per second (~25 miles per hour) in consultation with regional fire personnel. Prescribed fires follow a set of weather prescriptions for when fires can occur (Table S2).

Contemporary wildfires (2000-2016, from CalFIRE FRAP) were used to parameterize fire spread and size from the Central Sierra Nevada in order to increase the sample size of fires. Mean annual fire area (in ha) for observed data was 117 hectares per year (SD = 309), for modeled data, the mean value was 122 hectares per year (SD = 210). In order to move from fire intensity to fire severity (to encompass the mortality associated with fire), five fire experts working in the LTB provided their estimates of mortality for varying species, age, and intensity combinations. More details about the parameterization of the fire extension are found in Scheller et al. (2019). Suppression effort and fire spread are calibrated at the same time in order to try to account for both forces in recreating the contemporary fire regime.

Insect modeling

A modified version of the Biological Disturbance Agent extension (Biomass BDA v.2.0) was used to simulate insect outbreaks. Outbreak locations are based upon the species host density at a given site and the presence of non-hosts reduce disturbance probability. However, unlike Kretchun et al. (2016), the trigger for an outbreak was changed to be responsive to climate signals. This is because for many beetle species climate influences outbreaks in three ways: low winter temperatures cause beetle mortality; year-round temperatures influence development and mass attack; and drought stress reduces host resistance. Here, we modeled climate influences as a function of drought and mean minimum winter temperature, recognizing that the full suite of climatic influences is necessary for a fully mechanistic model. So long as annual climatic water deficit exceeded a set threshold, in conjunction with mean winter minimum temperatures exceeded a certain threshold, outbreaks could occur. A comparison between the modeled and observed outbreak dataset (USFS Aerial Detection Survey: https://www.fs.fed.us/foresthealth/applied-sciences/mapping-reporting/index.shtml) found an overestimation of frequency of occurrence but an underestimation of area impacted by insects (Figure S7).

Supplemental Tables:

Table S1. Suppression effort levels and effectiveness on fire spread probability.

	Fire Weather Index Thresholds		**Effort Level**		
Fire Type	Low-mod	Mod-high	Low	Moderate	High
Accidental	40	60	0	5	10
Lightning	40	60	0	5	10
Rx	40	60	0	0	0

Table S2. Prescribed fire parameters used for Scenario 5

Prescribed Fire Parameters	
MaximumRxWindSpeed	6.6 (m/s)
MaximumRxFireWeatherIndex	55 (unitless)
MinimumRxFireWeatherIndex	10 (unitless)
MaximumRxFireIntensity	1 (low)
NumberRxAnnualFires	364 (days of year allowable, subject to climate constraints)
FirstDayRxFires	1 (first julian day for allowable fire, subject to climate constraints)
TargetRxSize	72 (hectares)

Name	Longevity	Sexual maturity age	Shade tolerance	Fire tolerance	Seed effective dispersal distance (meters)	Maximum dispersal distance (meters)	Vegetative Reproduction Probability	Minimum age veg reproduction	Maximum age veg reproduction	Post-fire regeneration
Pinus jeffreyi	500	25	2	5	50	300	0	0	0	none
Pinus lambertiana	550	20	3	5	30	400	0	0	0	none
Calocedrus decurrens	500	30	3	5	30	1000	0	0	0	none
Abies concolor	450	35	4	3	30	500	0	0	0	none
Abies magnifica	500	40	3	4	30	500	0	0	0	none
Pinus contorta	250	7	1	2	30	300	0	0	0	none
Pinus monticola	550	18	3	4	30	800	0	0	0	none
Tsuga mertensiana	800	20	5	1	30	800	0.0005	100	800	none
Pinus albicaulis	900	30	3	2	30	2500	0.0001	100	900	none
Populus tremuloides	175	15	1	2	30	1000	0.9	1	175	resprout
Non-N fixing, Resprouting	80	5	2	1	30	550	0.85	5	70	resprout
Non-N fixing, Seeding	80	5	2	1	30	1000	0	0	0	none
N fixing, Resprouting	80	5	1	1	30	500	0.75	5	70	resprout
N fixing, Seeding	80	5	1	1	30	800	0	0	0	none

Table S3. Species parameters used in modeling.

Supplemental Figures:

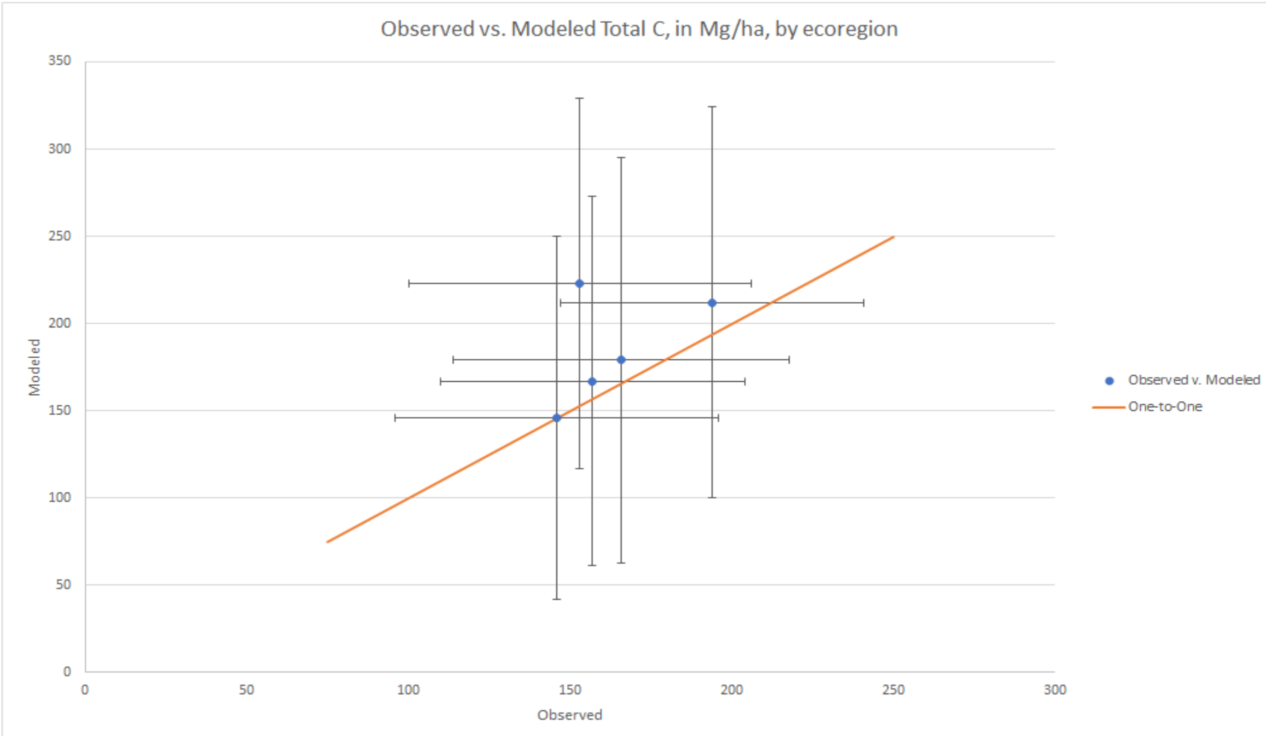

Figure S1. Observed versus modeled total C, in megagrams C per hectare, by ecoregion, error bars represent +/- 1 standard deviation.

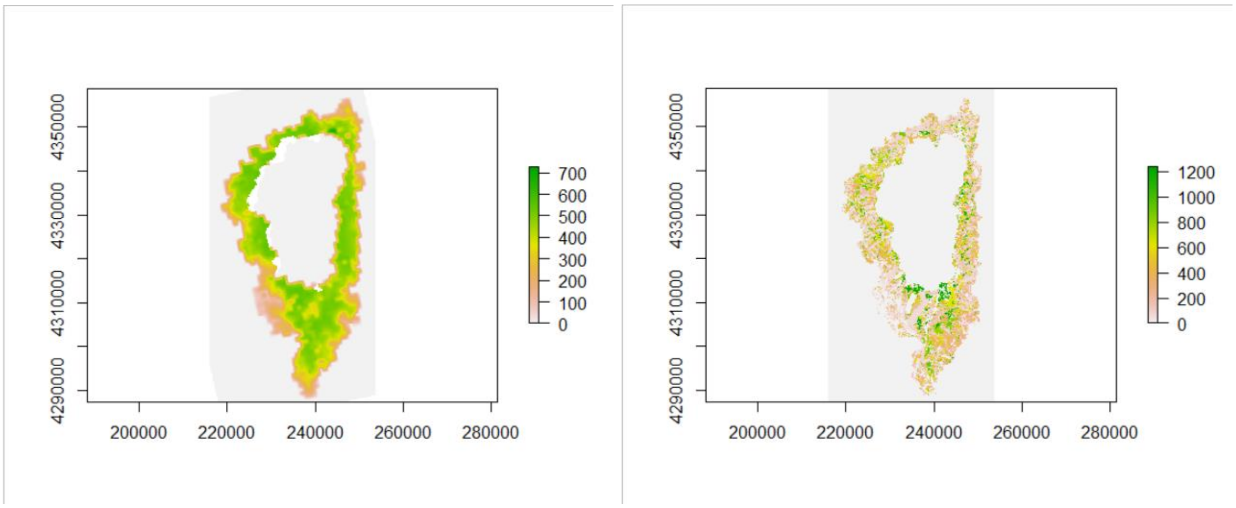

Figure S2. Comparison of MODIS (left) and LANDIS (right) estimates of Net Primary Productivity in g C/m ^2. Mean landscape value for MODIS was 393 g C/m ^2 (sd 134), while for LANDIS the mean value was 320 g C/m^2 (sd 312).

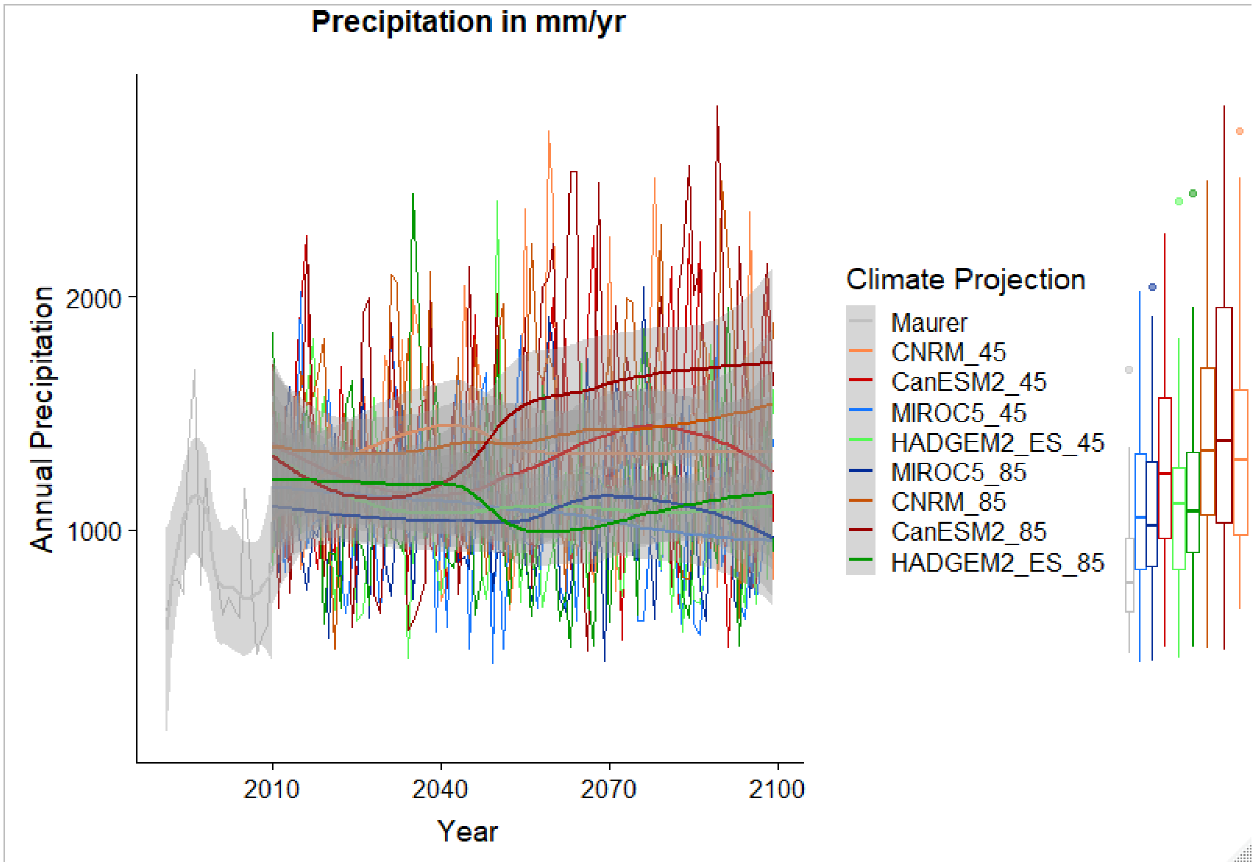

Figure S3. Projected precipitation in mm yr^{-1}, lines of best fit are GAM estimated, and boxplots represent distribution of annual precipitation for the years 2090-2100.

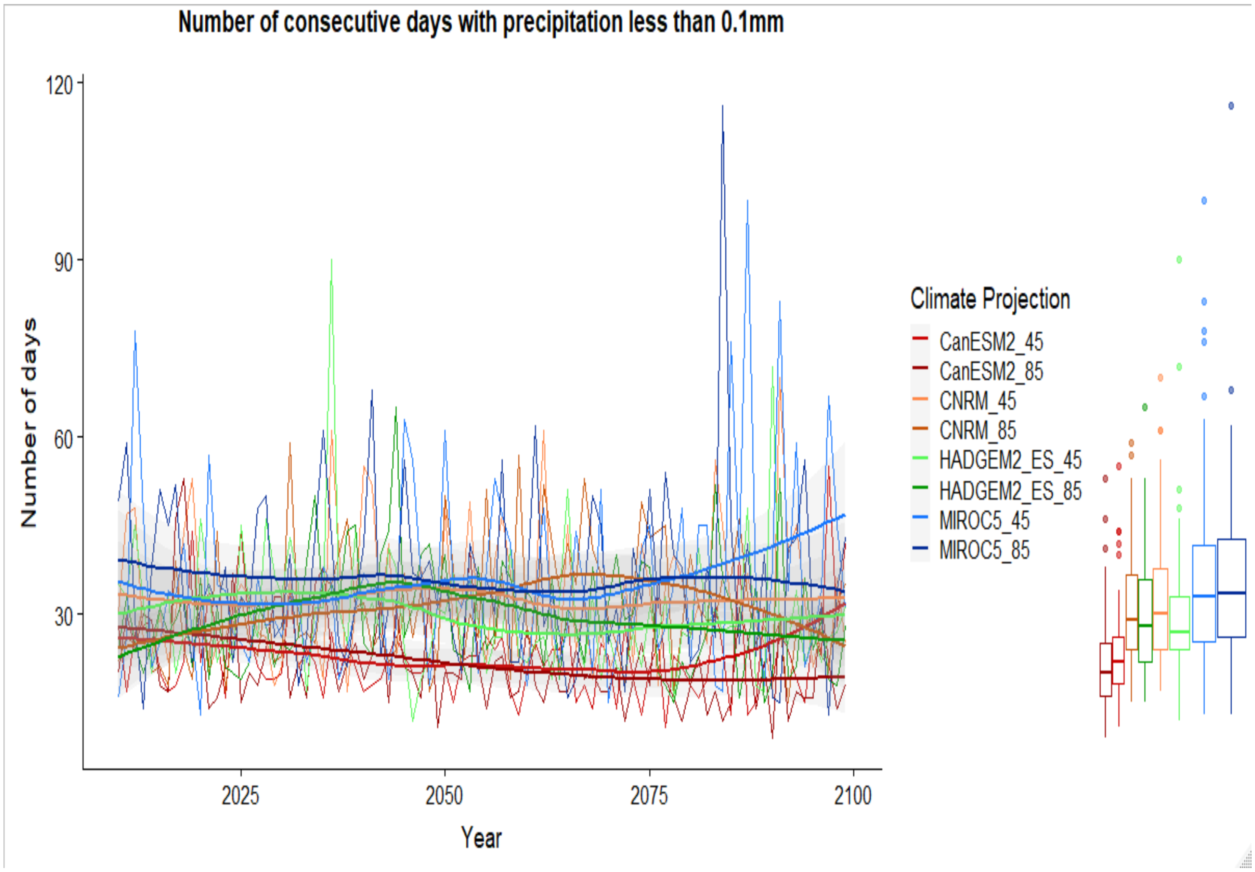

Figure S4. Projected number of consecutive days with no precipitation, lines of best fit are GAM estimated, and boxplots represent distribution of consecutive days per year for the years 2090-2100.

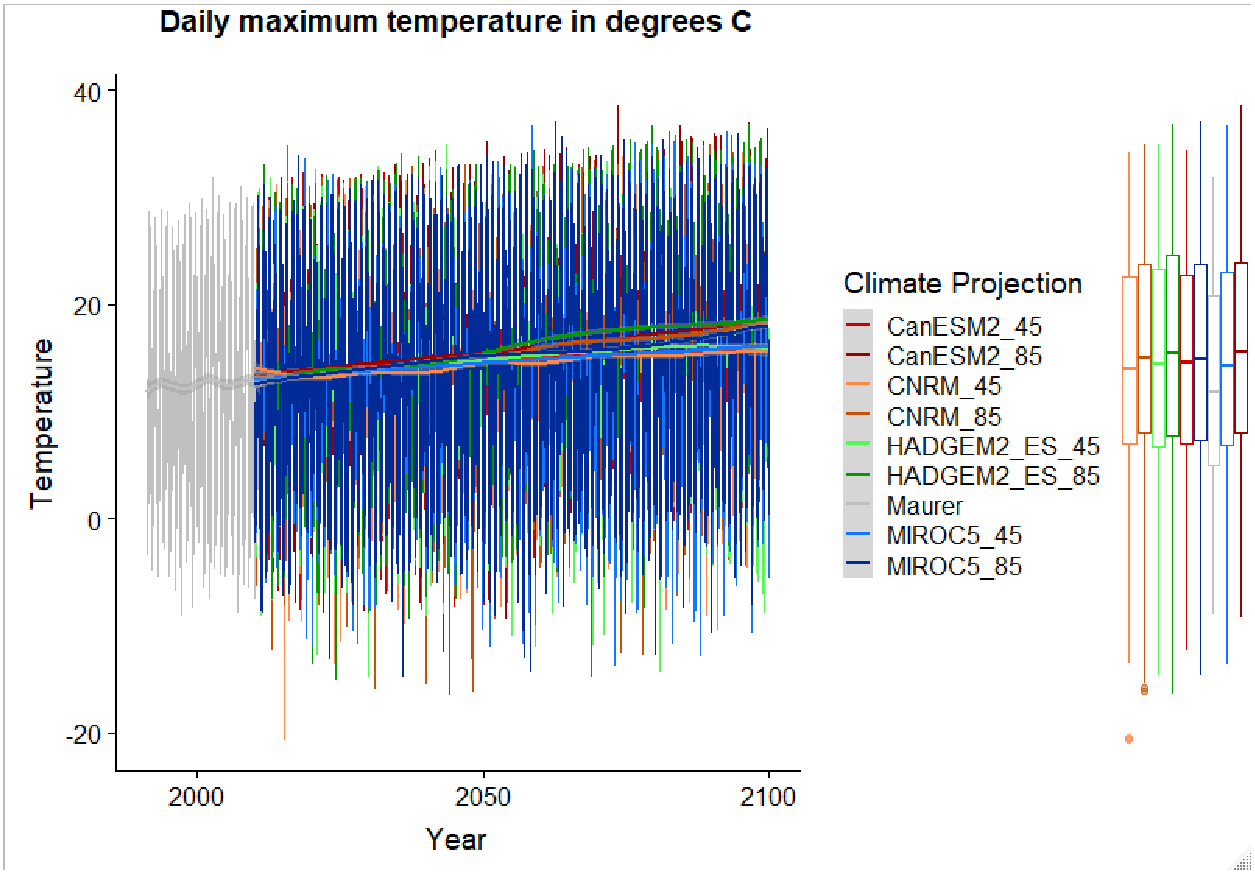

Figure S5. Projected daily maximum temperature in degrees C, lines of best fit are GAM estimated, and boxplots represent distribution of daily temperatures for the years 2090-2100 for the future climate projections.

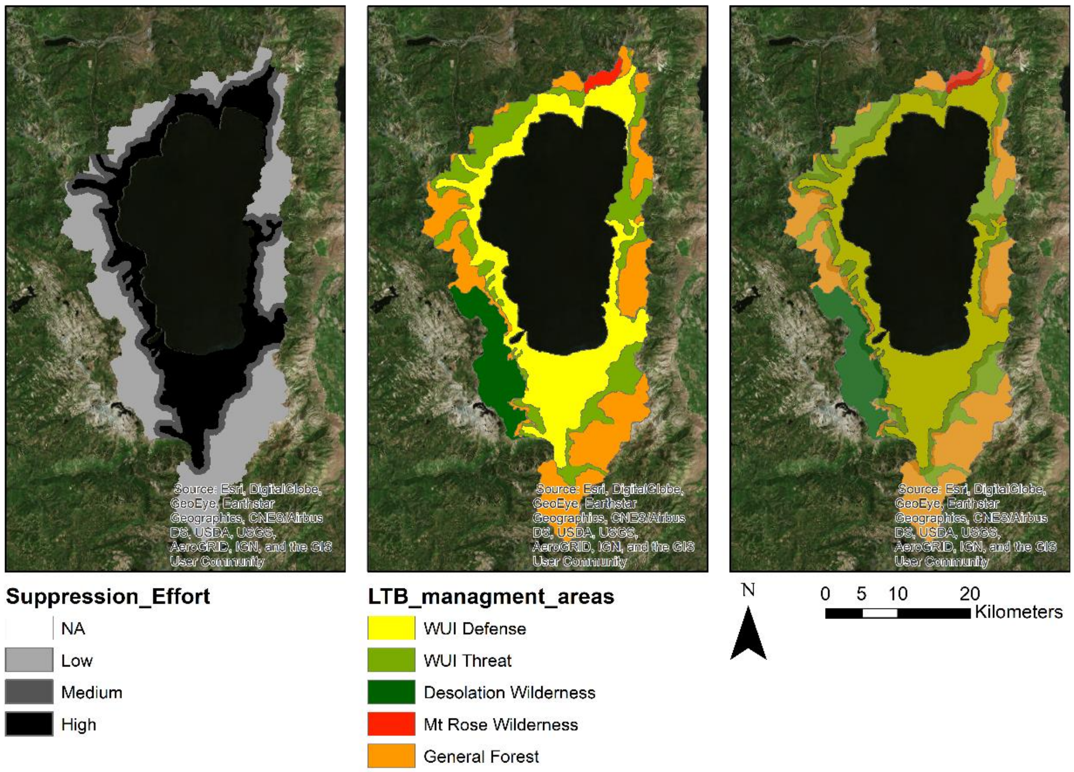

Figure S6. Map of suppression effort and management zone.

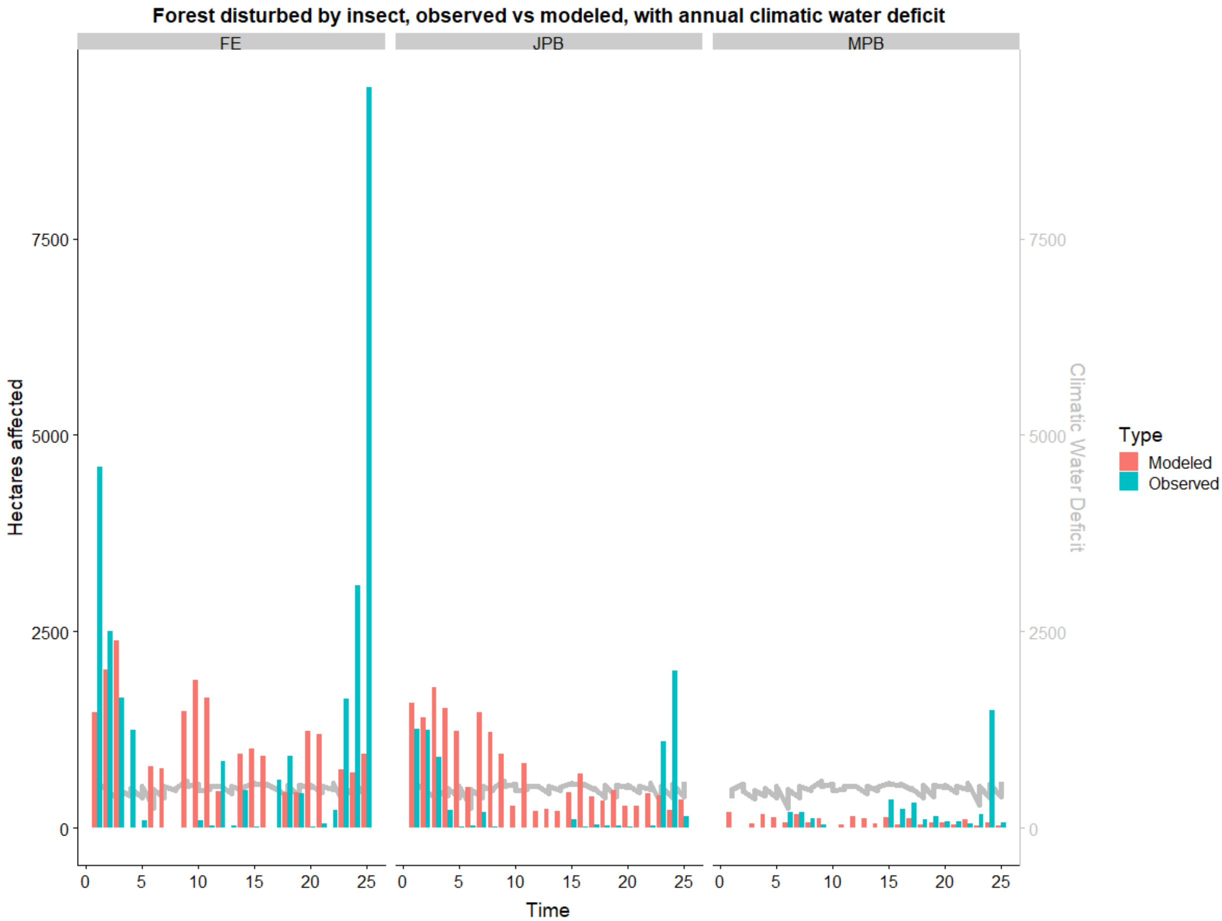

Figure S7. Observed versus modeled number of hectares affected by insect/mortality agent.

References

Kretchun, A. M., Loudermilk, E. L., Scheller, R. M., Hurteau, M. D., & Belmecheri, S. (2016). Climate and bark beetle effects on forest productivity—linking dendroecology with forest landscape modeling. *Canadian Journal of Forest Research*, 46(8), 1026-1034. https://doi.org/10.1139/cjfr-2016-0103

Parton, W.J., D.W. Anderson, C.V. Cole, J.W.B. Stewart. 1983. Simulation of soil organic matter formation and mineralization in semiarid agroecosystems. In: Nutrient cycling in agricultural ecosystems, R.R. Lowrance, R.L. Todd, L.E. Asmussen and R.A. Leonard (eds.). The Univ. of Georgia, College of Agriculture Experiment Stations, Special Publ. No. 23. Athens, Georgia.

Pierce, D.W., Cayan, D.R. and Dehann, L., 2016. Creating climate projections to support the 4th California climate assessment. University of California at San Diego, Scripps Institution of Oceanography: La Jolla, CA, USA.

Scheller, R., Kretchun, A., Hawbaker, T. J., & Henne, P. D. (2019). A landscape model of variable social-ecological fire regimes. *Ecological Modelling*, 401, 85-93. https://doi.org/10.1016/j.ecolmodel.2019.03.022

Scheller, R.M., Spencer, W.D., Rustigian-Romsos, H., Syphard, A.D., Ward, B.C. and Strittholt, J.R., (2011). Using stochastic simulation to evaluate competing risks of wildfires and fuels management on an isolated forest carnivore. *Landscape Ecology*, 26(10), 1491-1504. https://doi.org/10.1007/s10980-011-9663-6